Mass spectrometric imaging of ginsenosides localization in *Panax ginseng* root

Shu Taira and Ryuzo Ikeda

Japan Advanced Institute of Science and Technology

School of Material Science 1-1 Asahidai, Nomi, Ishikawa 923-1292, Japan

Naohiko Yokota

Waters Corporation 1-3-12 Kitashinagawa, Shinagawa, Tokyo 140-0001, Japan

Issey Osaka

Japan Advanced Institute of Science and Technology, Center for Nano Materials and Technology, 1-1 Asahidai, Nomi, Ishikawa 923-1292, Japan

Manabu Sakamoto and Mitsuro Kato

Nitto Analytical Techno-Center Co., Ltd. 1-1-2 Shimohozumi, Ibaraki, Osaka 567-8680, Japan

Yuko Sahashi

Nitto Denko Corporation 1-1-2 Shimohozumi, Ibaraki, Osaka 567-8680, Japan

Numbers of pages: 14

Numbers of figures: 3

Correspondence to: Dr. Yuko Sahashi, Nitto Denko Corporation 1-1-2 Shimohozumi, Ibaraki, Osaka 567-8680, Japan. Tel: (+81)761-51-1682, Fax: (+81)761-51-1682, e-mail: yuuko_sahashi@gg.nitto.co.jp

Abstract: We succeeded in performing mass spectrometric imaging (MSI) of the localization of ginsenosides (Rb_1, Rb_2 or Rc, and Rf) in cross-sections of the *Panax ginseng* root at a resolution of 100 μm using matrix-assisted laser desorption/ionization mass spectrometry (MALDI-MS). Tandem mass spectrometry (MS/MS) of alkali metal-adducted ginsenoside ions revealed structural information of the corresponding saccharides and agricones. MALDI-MSI confirmed that localization of ginsenosides in the cortex and the periderm is higher than that in the medulla of a lateral root. In addition, it revealed that localization of ginsenosides in a root tip (diameter, 2.7 mm) is higher than that in the center of the root (diameter, 7.3 mm). A quantitative difference was detected between localizations of protopanaxadiol-type ginsenoside (Rb_1, Rb_2, or Rc) and protopanaxatriol-type ginsenoside (Rf) in the root. This imaging approach is a promising technique for rapid evaluation and identification of medicinal saponins in plant tissues.

Key words

Ginsenosides, mass spectrometry, imaging, *Panax ginseng*, parenchyma

Introduction

The root of *Panax ginseng* C.A. Meyer is an important constituent of traditional Chinese medicine. Many pharmacological properties of the glycoside ginsenoside have been reported. There are numerous reports on the effects of glycoside ginsenoside on the central nervous system (Zhang et al., 1990; Zhang et al., 2008; Kim et al., 1998), relief of a pain (Nah et al., 2000), anti-tumor (Musende et al. 2009), ant-fatigue (Tang et al., 2008), anti-stress (Tachikawa et al., 2004), improvement of diabetes (Lee et al., 2006; Kang et al., 2008) and hypertension (Cai et al., 2009) and other activities (Lü et al., 2009). The presence and content of ginsenosides in *Panax ginseng*

has been studied in detail. The ginsenoside content in root extracts of *Panax ginseng* have been determined using liquid chromatography/electrospray ionization mass spectrometry (LC/ESI-MS), which includes complicated pretreatment; there is little knowledge of ginsenoside localization in root tissues (Li et al., 1996; Fuzzati et al., 1999; Cui et al., 2000; Tawab et al., 2003). Information on ginsenoside localization is vital.

In order to detect the presence of molecules of interest such as protein and DNA molecules in animal and plant tissues, researchers have treated tissues with the corresponding antibodies conjugated with labeling markers (in the case of protein molecules) and complementary DNA (cDNA) conjugated with probes (in the case of DNA molecules) (Komatsu et al., 1999; Shan et al., 2001; Tanaka et al., 2007; Morinaga et al., 2006). In order to facilitate increased direct visualization of biomolecules during biological analysis, mass spectrometry is used to distinguish individual molecules from each other. Mass spectrometric imaging (MSI) enables simultaneous detection of multiple analytes even in the absence of the target-specific markers such as antibodies (Fig. 1a) (Stoeckl et al., 2001; Taira et al., 2008). Matrix-assisted laser desorption/ionization time-of-flight mass spectrometry (MALDI-TOF-MS) has been commonly used for such analysis. MALDI is a soft ionization technique used in mass spectrometry (MS) in which a chemical matrix is used to assist the ionization of the analyte and to determine the structure followed by tandem mass spectrometry (MS/MS) (Nielsen et al., 2002).

Visualization of glycosides present in plant tissues is a new and useful technique in screening of plants that have high pharmacological activities that are traditionally used in Chinese medicine. However, there are no studies that report on direct imaging of compounds with pharmacological activity such as the *Panax ginseng* saponins. Our study is the first to report on the visualization of ginsenoside localization in the *Panax ginseng* root using MALDI-MSI. The naturally occurring ginsenosides in the cross-section of the root were identified by MS/MS and visualized at a

resolution of 100 μm using the MALDI-MSI technique.

Materials and Methods

Preparation of frozen cross-sections of Panax ginseng roots

Panax ginseng roots were purchased from Zen-Noh, Japan. After 6 years of cultivation at Daikonjima in Japan, the roots were harvested in 2008; the harvested roots were stored at 4°C until further use. Sample pieces for MALDI-MSI were cut from the center and tip of the lateral root body using a blade and the resultant frozen sample piece axially set in a cryostat (RV-240; Yamato Kohki, Japan) at –16 °C. Next, they were cut into serial sections (50 μm) and thaw-mounted on glass slides for MSI and toluidine blue (TB) staining, respectively. The glass slides with the sections were immersed in 0.1% TB solution for 10 s to stain the nucleus and the cytoplasm and then washed with tap water for 5 min. The stained sections were sealed with coverslips by using Entellen reagent. These TB-stained sections were used to determine various regions of the lateral root tissue (xylem, cortex, and periderm).

MALDI-MSI of ginsenoside localization in Panax ginseng roots

The efficacy of MSI in MS was confirmed by a MALDI-quadrupole (Q)-TOF instrument (Synapt High Definition MS; Waters, USA) using yttrium aluminium garnet (YAG laser) emissions at 355 nm. Purified ginsenosides, Rb_1, Rb_2, Rc, Rf, and Rg_1 (Funakoshi, Japan) dissolved in 70% methanol (Wako Pure Chemicals, Japan) were employed as standards. Saturated α-cyano-4-hydroxyciannamic acid (CHCA) (Sigma, USA) was dispersed in 1 mL of 10 mM methanolic solution of sodium iodide. The suspension was centrifuged, and the supernatant fluid was sprayed on a glass slides with the sections using an airbrush (nozzle caliber, 0.2 mm), while the CHCA matrix solution (10 $mg \cdot mL^{-1}$ CHCA, 70% methanol) was applied to another section. The

section surface was irradiated with 100 laser shots in the positive ion detection mode of the mass spectrometer. In order to detect the laser spot area, the sections were scanned and laser spot areas (66 × 77 spots) and (34 × 42 spots) were detected with a spot-to-spot center distance of 100 μm in each direction at the center and the tip of the root, respectively. The tissue surface was irradiated with 100 laser shots in the positive ion detection mode. For each xylem, cortex and periderm areas, related intensities were processed by discarding peaks with back ground. The remaining intensities constituted the set of variables that was used for statistical analysis.

Results and Discussion

A number of high-intensity signals, including those of ginsenosides, were detected in the mass spectrum obtained from the root seeped with CHCA in the presence of sodium ion (Fig. 1b). The root sections were subjected to MS/MS for identification of respective ginsenosides based on structural analysis. Three signals $[M+Na]^+$ ion at *m*/*z* 823.5, $[M+K]^+$ ion at *m*/*z* 1117.5, and $[M+K]^+$ ion at *m*/*z* 1147.5 corresponding to those of ginsenoside (G)-Rf or G-Rg_1, G-Rb_2 or G-Rc, and G-Rb_1, respectively, were obtained. The MS/MS spectrum of G-Rf showed a specific pattern of the precursor ion at *m*/*z* 823.5 and the sole derivative ion at *m*/*z* 381.4 that corresponds to that of the disaccharide moiety of G-Rf (Fig. 2a). No difference was detected between the MS/MS spectra of G-Rb_2 and G-Rc, which had the same exact mass; the precursor ion was detected at *m*/*z* 1117.5, and 2 derivative ions $[y1+K]^+$ and $[z1+K]^+$ were detected at *m*/*z* 351.1 corresponding to the disaccharide moiety of R_2 and *m*/*z* 805.4 corresponding to the agricone and disaccharide moieties of R_3, respectively. The difference between G-Rb_2 and G-Rc is due to the arabinose conformation (arabinopyranose for G-Rb_2 and arabinofuranose for G-Rc) within the disaccharide moiety of R_2, thus rendering it difficult to distinguish between G-Rb_2 and G-Rc using the MS/MS technique (Fig. 2b). Although we did not determine which disaccharide was desorbed, the spectra of G-Rb_2 and

G-Rc suggest that the cleavage of the sugar moiety at position R_2 is likely to occur easily than at position R_3. The MS/MS spectrum of G-Rb_1 revealed the precursor ion at *m*/*z* 1148.5 and 2 derivative ions $[y1+K]^+$ at *m*/*z* 381.1 corresponding to the disaccharide moiety of R_2 or R_3 and $[z1+K]^+$ at *m*/*z* 805.4 corresponding to the agricone and disaccharide moieties of R_2 or R_3. In addition, we confirmed that these MS/MS spectra correspond to those of the standard ginsenosides, G-Rf or G-Rg_1 (Exact MS (Me) 800.5), G-Rb_2 or G-Rc (Me 1078.6), and Rb_1 (Me 1108.6) showing alkali metal-adducted forms as respective precursor ions (data not shown).

Signals corresponding to ginsenosides in the MS/MS spectra showed respective ionized forms to be predominantly alkaline metal adducts such as potassium and sodium (*m/z* 823.5 and 1117.5 and 1148.5). No $[M+H]^+$ ion was detected due to an abundance of potassium and sodium ions in plant tissues. With the addition of sodium iodide in the matrix solution, the signal of G-Rf (*m/z* 823.5) was detected as a sodium adduct. Conversely, even with the addition of sodium iodide in the matrix solution, the signals of G-Rb_2 and G-Rc (*m/z* 1117.5) and Rb_1 (*m/z* 1147.5) were detected as potassium adducts. The concentration of potassium ions in plant tissues is 10-fold more than that of sodium ions. The optimal ionization of ginsenosides varies in different species.

Next, we performed MALDI MSI with the root samples of *Panax ginseng*. Successive lateral root sections were stained with TB for identifying the regions where MSI was performed. We prepared sections from the center and the tip of the lateral root (Fig. 3a); further, the xylem, cortex, and periderm regions of the root were defined (Fig. 3b). In the reconstituted MS image, distinct ginsenoside localizations were observed at *m/z* 823.5 (G-Rf: $[M+Na]^+$) (Fig. 3c), 1117.5 (G-Rb_2 or G-Rc: $[M+K]^+$) (Fig. 3d), and 1147.5 (G-Rb_1: $[M+Na]^+$) (Fig. 3e). These images revealed the concentration of the ginsenosides in the periderm and a part of the cortex in the center of the root and the entire tip. In contrast, lower MS intensities were observed in the xylem. High MS intensity was detected radially in the cortex, suggesting that this portion consisted of living cells, i.e. the

radial parenchyma. Radial parenchyma is involved in transport and storage of nutrient elements and production of secondary metabolites. In this case, we hypothesize that the image result reveals the storage of glycosides as a secondary metabolite in the radial parenchyma.

A semiquantitative analysis was performed by correlating the MS intensities and root layer structures. For the total MS intensity per unit area, we detected that MS intensity at the center of the root was lower than that at the root tip. Significant difference between the MS intensities at the center and the tip of the root was detected at the *m/z* value 1117.5. (Fig. 3f).

Next, we evaluated the localizations of ginsenosides in the xylem, cortex, and periderm (Fig. 3g inset). We detected that ginsenosides were unevenly distributed in the periderm and were more abundant in the tip region as compared to the central region. At the *m/z* value 823.5, the periderm contained greater amounts of G-Rf than the inner portion of the root. Although low MS intensity was detected at the center of the root, a significant difference was detected between MS intensity in the xylem and the cortex or periderm. However, at an *m/z* value of 1117.5, no significant difference was detected between MS intensities in different regions at the center of the root. A significant difference was detected between MS intensities in the xylem and the periderm at the tip of the root. At an *m/z* value of 1147.5, as compared to the xylem at the center and tip of the root, greater amounts of G-Rb_1 were detected in the cortex and the periderm both at the center and the tip of the root, although no significant difference was observed from every assortment.

In particular, ginsenosides are maldistributed in the periderm and the tip region of the root (Shan et al. 2006). Previous studies have reported the estimation of ginsenoside concentrations in each region of the root using gas chromatography; these reports revealed that G-Rbc groups were concentrated to a greater extent in the lateral root (Tani et al. 1981). This finding is consistent with the observations made from the ion image of ginsenosides in our study. In addition, we found that ginsenosides were similarly localized in the radial parenchyma in the cortex and the periderm.

Conclusion

MALDI-MS is an effective technique for the identification and visualization of ginsesonides in the *Panax ginseng* root. Ginsenosides preferably existed toward the outer portion and tip of the lateral root; the G-Rbc group was found to be more dominantly distributed than the G-Rf group. MALDI-MS imaging is a direct and easy-to-use technique for the determination of target molecule localization without any marker. This method can be applied to a new screening method of raw plants or plant cells lilke callus that possess a high pharmacological activity, new quality evidence system of food, and new evaluation method of plant cultivation or cell culture. In future, we intend to obtain an effective spatial resolution image by nanoparticle-assisted laser desorption/ionization (nano-PALDI) MS imaging to reveal a more accurate distribution of molecules such as their cellular resolution (Taira et al., 2008) and the selection and culture of high pharmaceutical activity regions in roots.

Acknowledgments

We thank member of Takagi and Takamura laboratory in JAIST, particularly Prof. M. Takagi and Prof. Y. Takamura, for providing technical assistance and advice. This research was supported by a WAKATE-B grant from the Japan Society for the Promotion of Science to S. T. and a Grant-in-Aid to S. T. from JAIST and the resource of coordinated research program to Nitto Denko.

References

Cai, B.X., X.Y. Li, J.H Chen, Y.B. Tang, G.L. Wang, J.G. Zhou, Q.Y. Qui, Y.Y. Guan. Ginsenosides-Rd, a new voltage-independent Ca^{2+} entry blocker, reverses basilar hypertrophic remodeling in stroke-prone renovascular hypertensive rats. *Eur. J. Pharmacol.* 606: 142-149, 2009.

Cui, M., F.Song, Y. Zhou, Z. Liu, S. Liu. Rapid identification of saponins in plant extracts by electrospray ionization multi-stage tandem mass spectrometry and liquid chromatography/tandem mass spectrometry. *Rapid Commun. Mass Spectrom.* 14: 1280–1286, 2000.

Cui, M., F.Song, Y. Zhou, Z. Liu, S. Liu. Metal ion adducts in the structural analysis of ginsenosides by electrospray ionization with multi-stage mass spectrometry. *Rapid Commun. Mass Spectrom.* 15: 586–595, 2001.

Fuzzati, N., B. Gabetta, K. Jayakar, R. Pace, F. Peterlongo.Liquid chromatography–electrospray mass spectrometric identification of ginsenosides in *Panax ginseng* roots *J. Chromato. A.*, 854: 69–79,1999.

Kang, K.S., N. Yamabe, H.Y. Kim, J.H. Park, T. Yokozawa. Therapeutic potemtial of 20(S)-ginsenoside Rg(3) against streptozotocin-induced diabetic renal damage in rats. *Eur. J. Pharmacol.* 591: 266-272, 2008.

Kim, D.H., J.S. Jung, H.W. Suh, S.O. Huh, S-K. Min, B.K. Son, J.H. Park, N.D. Kim, Kim, H.S. Yung, K. Dong. Inhibition of stress-induced plasma corticosterone levels by ginsenosides in mice: involvement of nitric oxide. *NeuroReport* 9: 2261-2264, 1998.

Komatsu, M., E. Kominami, K. Arahata, T. Tsukahara. Cloning and characterization of two neural-salient serine/arginine-rich (NSSR) proteins involved in the regulation of alternative splicing in neurons. *Genes to Cells* 4: 593-606, 1999.

Lee, W.K., S.T. Kao, I.M. Liu, J.T. Chen. Increase of insulin secretion by ginsenoside Rh2 to lower plasma glucose in Wistar rats. *Clin. Exp. Pharmacol. Physiol.* 33: 27-32, 2006.

Li, T.S.C., G. Mazza, A.C. Cottrell, L. Gao. Ginsenosides in Roots and Leaves of American Ginseng. *J. Agric. Food Chem.* 44: 717-720, 1996.

Lü, J.M., Q. Yao, C. Chen. Ginseng compounds: an update on their molecular mechanisms and medical applications. *Curr. Vasc. Pharmacol.* 7: 293-302, 2009.

Morinaga, O., H. Tanaka, Y. Shoyama. Detection and quantification of ginsenoside Re in ginseng samples by a chromatographic immunostaining method using monoclonal antibody against ginsenoside Re. *J. Chromatogr. B*, 830, 100–104, 2006.

Musende, .A.G, A. Eberding, C. Wood, H. Adomat, L. Fazli, A. Hurtado, W. Jia, M.B. Bally, E.T. Guns. Pre-clinical evalution of Rh2 in PC-3 human xenograft model for prostable cancer in vivo: formation, pharmacokinetics, biodistribution and efficacy. *Cancer Chemother Pharmacol.* 64: 1085-1095, 2009.

Nah J.J., J.H. Hahn, S. Chung, S.Choi, Y. I. Kim, S.Y. Nah. Effect of ginsenosides, active components of ginseng, on capsaicin-induced pain-related behavior. *Neuropharmacology* 39: 2180-2184, 2000.

Nielsen, M.L., K.L. Bennett, B. Larsen, M. Moniatte, M. Mann. Peptide End Sequencing by Orthogonal MALDI Tandem Mass Spectrometry. *J. Proteome Res.* 1: 63-71, 2002.

Shan, S., H. Tanaka, Y. Shoyama. Enzyme-linked immunosorbent assay for glycyrrhizin using anti-glycyrrhizin monoclonal antibody and an eastern blotting technique for glucuronides of glycyrrhetic acid. *Anal. Chem.* 73: 5784-5790. 2001.

Stoeckli, M., P. Chaurand, D.E. Hallahan, R.M. Caprioli. Imaging mass spectrometry: a new technology for the analysis of protein expression in mammalian tissues. *Nature Med.* 7: 493–496, 2001.

Tachikawa, E., K. Kudo. Proof of the mysterious efficacy of ginseng: basic and clinical trials: suppression of adrenal medullary function in vitro by ginseng. *J. Pharmacol. Scil.* 95: 140-144, 2004.

Taira, S., Y. Sugiura, S. Moritake, S. Shimma, Y. Ichiyanagi, M. Setou. Nanoparticle-Assisted Laser Desorption/Ionization Based Mass Imaging with Cellular Resolution. *Anal. Chem.* 80: 4761-4766, 2008.

Tanaka, H., N. Fukuda, Y. Shoyama. Eastern blotting immunoaffinity concentration using monoclonal antibody for ginseng saponins in the field of traditional cheinese medicines. *J. Agric. Food Chem.* 55: 3783-3787, 2007.

Tang, W., Y. Zhang, J. Gao, X. Ding, S. Gao. The anti-fatigue effect of 20(R)-ginsenoside Rg3 in mice by intransally administration. *Biol. Pharm. Bull.* 31: 2024-2027, 2008.

Tani, T., M. Kubo, T. Katsuki, M. Higashino, T. Hayashi, S. Arichi. Histochemistry II ginsenosides in ginseng (*Panax ginseng* root). *J. Nat. Prod.* 4: 401-407, 1981.

Tawab, M.A., U. Bahr, M. Karas, Mwurglics, M. Schubert-Zsilavecz. Degradation of ginsenosides in humans after oral administration. *Drug Metabol. Dispos.* 31: 1065-1071, 2003.

Zhan, G., A. Liu, Y. Zhou, X. San, T. Jin, Y. Jin. Ginsenoside-Rg2 protects memory impaiment via anti-apoptpsis in a rat model with vascular dementia. *J. Ethnopharmacol.* 115: 441-448, 2008.

Zhan, J.T., Z.W. Que, Y. Liu and H.L. Deng, Preliminary study on antioamnestic mechanism of ginsenoside Rg1 and Rb1. *Clin. Med. J.* 103: 932-938, 1990.

Figure legends

Figure 1

Schematic illustration of mass spectrometric imaging (MSI) (a), Matrix-assisted laser desorption/ionization (MALDI)-mass spectra of *Panax ginseng* root (b)

Figure 2

Matrix-assisted laser desorption/ionization (MALDI) tandem mass spectra of ginsenoside (G)-Rf (a), G-Rb_2 or Rc (b), and G-Rb_1 (c) from the section of raw *Panax ginseng* root. glc: β-D-glucose, arap: β-D-xylopranosyl (pyranose), and araf: α-L-alabinofuranosyl (furanose)

Figure 3

Matrix-assisted laser desorption/ionization (MALDI)-mass spectrometric imaging (MSI) of ginsenosides. Optical images of toluidine blue-stained *Panax ginseng* sections (a). The region and ratio of area of lateral root (b). MS spectra reconstructed as ion images for *m/z* 823.5 (c), *m/z* 1117.5 (d), and *m/z* 1147.5 (e). Total MS intensity at the center and tip of *Panax ginseng* root (f). Areas enclosed within the dash-lined rectangles in (g) were measured to quantify the MS intensity across the xylem (X), cortex (C), and periderm (P) regions. Obtained values were commuted to per unit area. The values are expressed in terms of mean ± SEM. $*P < 0.05$ and $**P < 0.01$ with Student's *t*-test. n = 2. The scale bar is 1 mm.

.

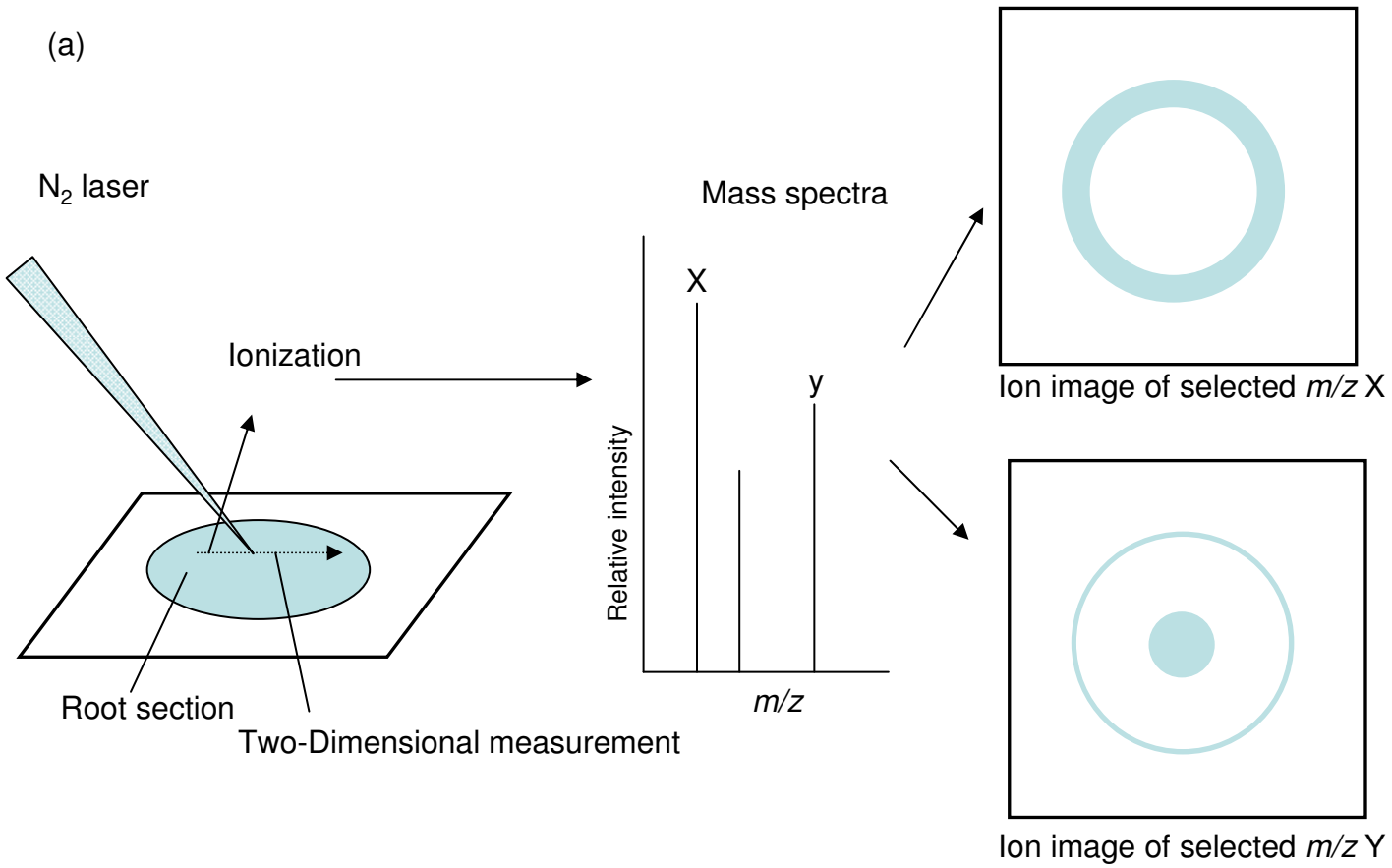

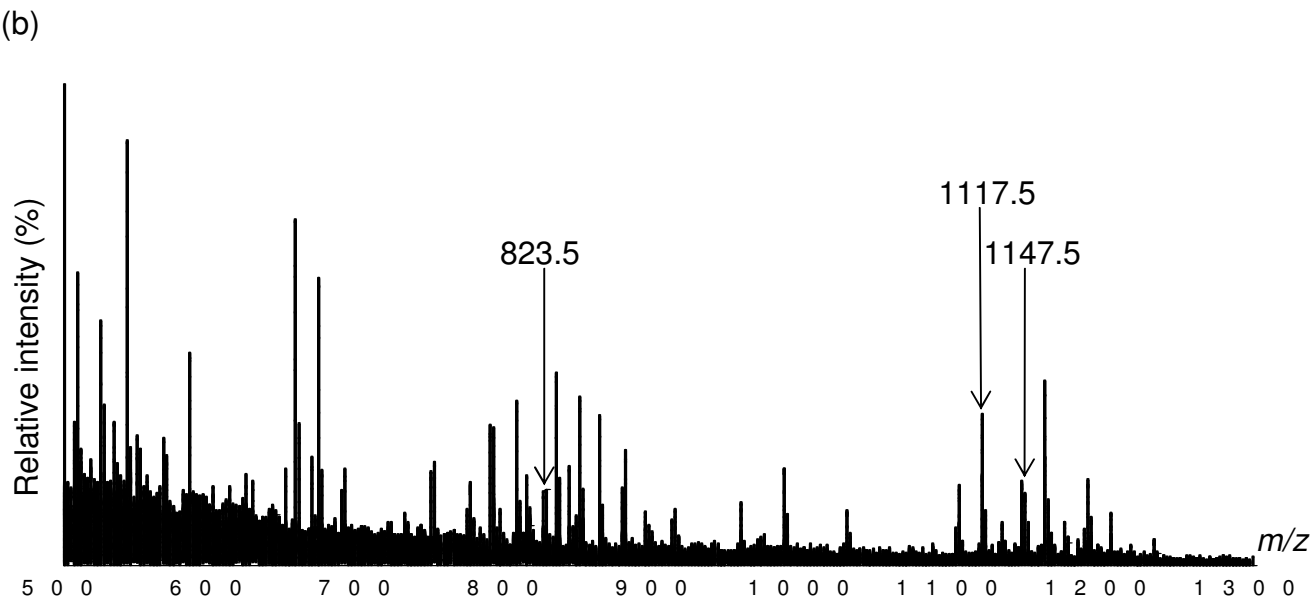

Figure 1 Taira et al.

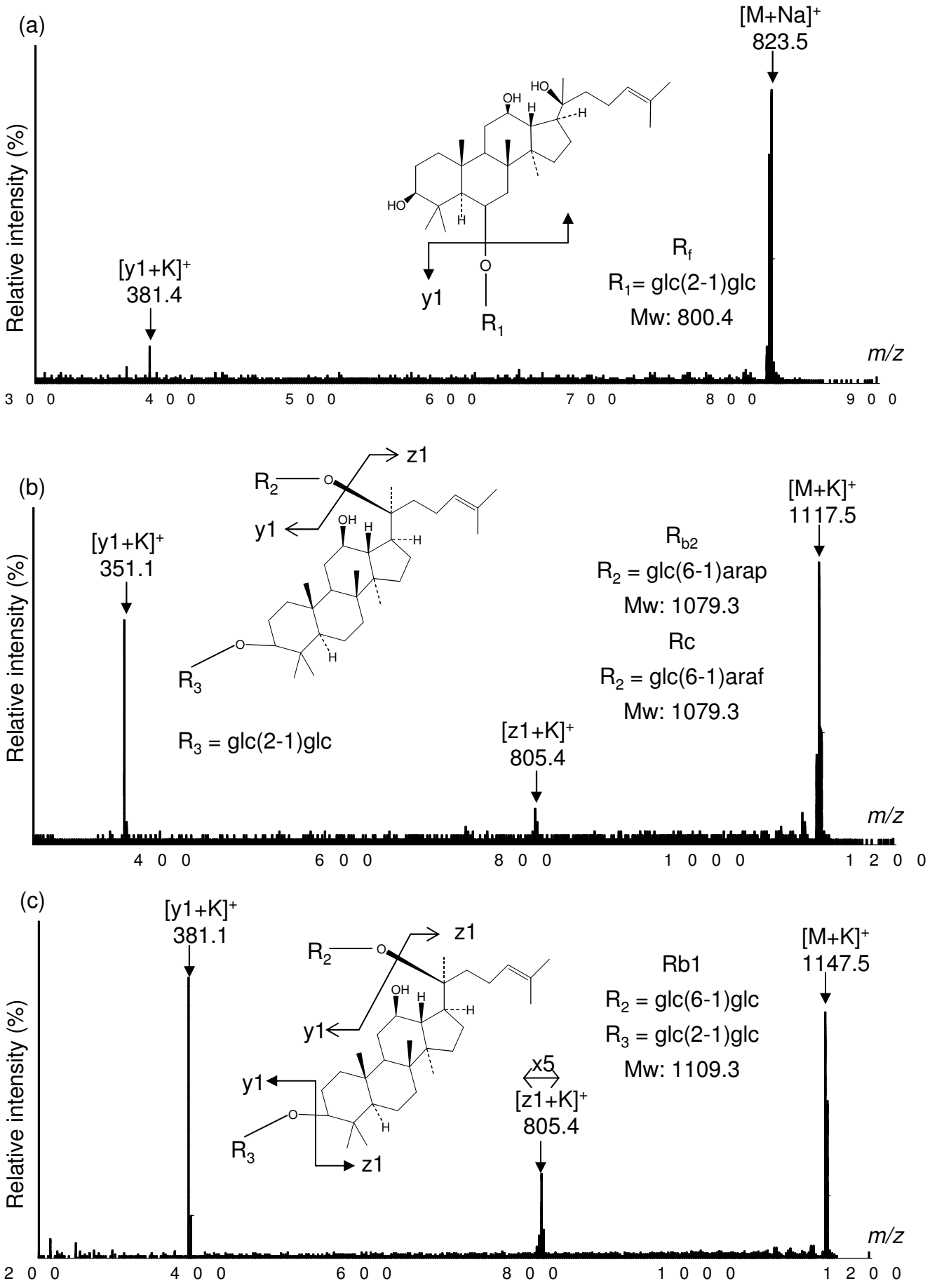

Figure 2 Taira et al.

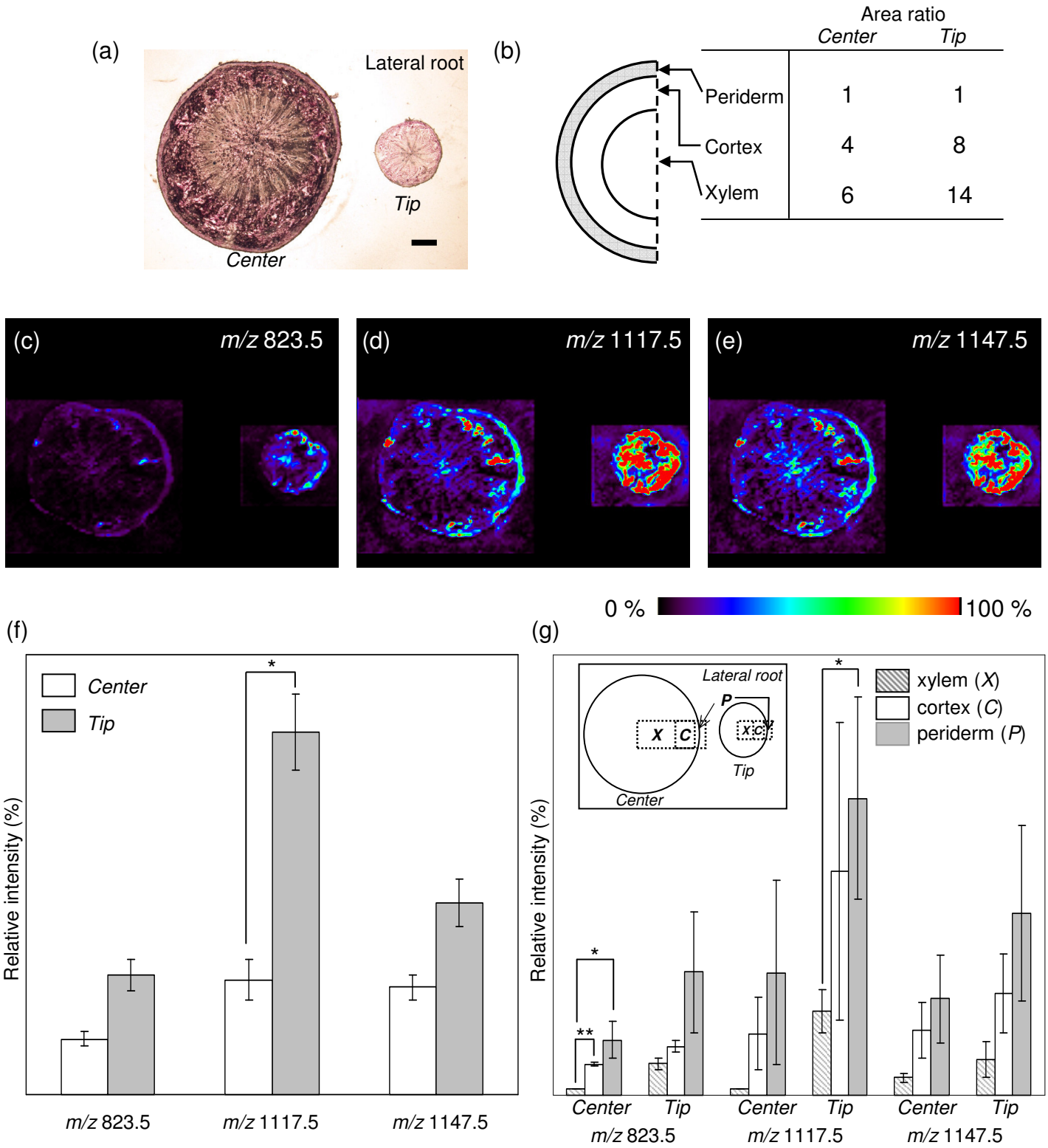

Figure 3 Taira et al.